Article:
Zhao, Y.-J., Zhang, Y.-K., Cui, Y. et al. (2022) Pinch combined with exergy analysis for heat exchange network and techno-economic evaluation of coal chemical looping combustion power plant with CO2 capture. Energy, 238 (Part A). 121720. ISSN: 0360-5442

https://doi.org/10.1016/j.energy.2021.121720

Pinch Combined with Exergy Analysis for Heat Exchange Network and Techno-economic Evaluation of Coal Chemical Looping Combustion Power Plant with CO_2 Capture

Ying-jie Zhao[a,c], Yu-ke Zhang[a], Yang Cui[a], Yuan-yuan Duan[a], Yi Huang[b], Guo-qiang Wei[d], Usama Mohamed[c,e], Li-juan Shi[b,c], Qun Yi[b,c,e]*, William Nimmo[e]*

[a]*Training Base of State Key Laboratory of Coal Science and Technology Jointly Constructed by Shanxi Province and Ministry of Science and Technology, Taiyuan 030024, PR China*

[b]*School of Chemical Engineering and Pharmacy, Wuhan Institute of Technology, Wuhan, 430205, P. R. China.*

[c]*College of Environmental Science and Engineering, Taiyuan University of Technology, Taiyuan 030024, P. R. China.*

[d]*Guangzhou Institute of Energy Conversion, Chinese Academy of Sciences (CAS), Guangzhou 510640, PR China*

[e]*Energy 2050 Group, Faculty of Engineering, University of Sheffield, S10 2TN, UK*

Abstract: A coal chemical looping combustion (CLC) power plant (600 MW) with CO_2 capture was established and validated. The key operation parameters and conditions for the coal chemical looping combustion process were tested and optimized. Heat exchange network (HEN) was established and optimized using the combined pinch and exergy analysis method for matching and integrating different levels or grade energy, from flue gas and exhaust steam waste heat, in coal chemical looping combustion power plant to maximize the energy efficiency output. Followed by conducting a techno-economic evaluation and exergy distribution analysis which showed that the net energy efficiency of the CLC power plant (34.8%, improved by 1.9%) is 2.4% higher than the monoethanolamine (MEA)-based ultra-supercritical coal power plant (32.4%) with the same CO_2 capture ratio (90%). The CLC power plant also provides a lower cost of electricity (0.088-0.127$ /kWh) and less coal consumption (381 g/kWh), compared to the MEA-based power plant (0.143 $/kWh, 408 g/kWh). The cost and energy penalty of CO_2 enrichment and separation are less when compared to traditional MEA-based ultra-supercritical coal power plants due to the intrinsic nature of in-suit CO_2 capture, the lower

*Corresponding author, Fax & Tel.: +86 3513176580. *E-mail address*: shilijuan@tyut.edu.cn (L.J, Shi); yiqun@tyut.edu.cn (Q, Yi)

exergy destruction in the chemical looping combustion process, and sufficient energy integration and recovery from HEN.

Keywords: chemical looping combustion, power plant, pinch and exergy analysis, CO_2 capture, techno-economic evaluation

1. Introduction

Nowadays, energy security and environmental pollution (especially CO_2 emissions) have gained much attention since these issues need to be addressed while meeting rapid economic growth. Fossil fuel-based power plants are under the spotlight for further improvement in efficiency and other factors, since approximately 39% [1] of global electricity is generated by coal. Therefore, increasing energy-saving and reducing carbon dioxide (CO_2) emissions have been suggested for coal power plants. Amongst the developments made in this field, technology innovation is of paramount significance as it guides through several technological developments for the reduction in CO_2 emissions from electric power plants.

Chemical looping combustion (CLC) is proposed due to its unique ability in energy-saving and CO_2 emission reduction [2, 3]. Instead of using molecular oxygen in conventional combustion, carbonaceous fuels in CLC processes are combusted using lattice oxygen in the form of a metal oxide [4], therefore avoiding CO_2 dilution since the flue gas is mainly composed of H_2O and CO_2. After the condensation of H_2O, almost pure CO_2 is obtained. As a result, avoiding the energy intensive carbon capture process, making CLC a suitable alternative for CO_2 capture. Additionally, another advantage is that CLC is less irreversible during combustion [5, 6]. In comparison with the conventional combustion process, CLC can reduce exergy loss during the combustion reaction, therefore improving its energy utilization, due to the stepwise utilization of energy. Based on the aforementioned merits of CLC, this novel technology can be applied for the environmentally benign power generation [7, 8]. Most of the studies on CLC-power plants mainly focus on gas turbine using gaseous fuels [9-12]. The use of solid fuels in CLC has been highly developed in the last decade and

is currently fully demonstrated in actual system application and can be applied in power plants [13-15].

Commonly, improving turbine inlet temperature and pressure can enhance power plant efficiency. There are two strategies mainly used to improve power generation efficiency in previous studies. One strategy involved improving the reactor temperature [9, 16-18] which has been widely investigated. Another strategy for power plant efficiency improvement is to change the CLC reactor pressure [19-21]. The thermal efficiency improvement of the heat exchange network is another aspect to enhance the power plant's thermal efficiency. Recently, mathematical programming methodology (a mixed integer nonlinear programming model) [22, 23], exergy analysis [24] and pinch analysis [25, 26], and a combined pinch and mathematical programming methodology [27] were also proposed to systematically integrate and optimize the heat exchange network of energy conversion systems. Pinch analysis is a systematic method that can be used to improve energy utilization in the HEN. The major limitation of pinch analysis is that it can only deal with heat transfer processes, but not the processes involving changes in pressure or compositions. Exergy analysis includes all stream properties (temperature, pressure, and composition) that can overcome the weakness of pinch analysis. Therefore, a new method, combining pinch and exergy analysis (CPEA) [28-30] is used to combine these two methods. Theoretically it can also clearly indicate the limitations to any improvement. Using the mentioned methodology we can simplify the present exergy destruction without the complexity mathematic model, an upgraded graphical tool, combined pinch-exergy analysis methodologies, is used for heat exchanger network design and optimization in ammonia refrigeration process [31], a gas-fired steam power plant [32], and a complex natural gas refinery [24]. This approach was applied to our process system to optimize the heat exchanger network.

The studies mentioned above paid attention on reducing the energy penalty and improving the energy efficiency of CLC power plants in different strategies and methods (adjustment of temperature or pressure in CLC reactors, or co-production system integration). However, few studies have focused

on heat exchange network design and optimization for matching of different energy levels from the two reactors in CLC power plants, which has a significant impact on power plant efficiency. The present study is motivated by recognizing this gap and conducting the following work. Firstly, matching energy between the heat source (combustion) and heat recovery, integration, and utilization. There are two heat energy flows generated from the CLC process (AR and FR), which are completely different from the traditional coal power plant with a single combustor. Secondly, to clarify the exergy distribution across the power plant. Henceforth, the objectives of this study are set as follows: (1) Establishment and validation of a detailed CLC-power plant with CO_2 capture process model, as well as key parameters optimization of coal CLC process; (2) heat exchange network model was established and optimized for matching and optimizing the different energy levels and heat recovery in CLC-power plant to maximize the energy efficiency; (3) analysis of the exergy destruction and distribution of CLC-power plant; (4) techno-economic analysis and evaluations. The results will be compared to traditional ultra-supercritical coal power plants to highlight the feasibility, potential and find out the key point for further improving the performance of CLC-power plants.

2. Process description

In this study, CLC-power plant with CO_2 capture is simulated using Aspen Plus V10.0 software. The process diagram of the coal CLC-power plant is shown in Fig. 1. The whole plant is divided into four sub-systems (CLC unit, heat recovery steam generator (HRSG), steam turbine (ST), and CO_2 capture and storage (CCS)). The coal used in this study is based on Illinois No. 6 bituminous coal [33] with a high heating value (HHV) equal to 27,113 kJ/kg. The proximate analysis results of coal at air-dried basis (wt.%) shows that it contains 11.2% moisture, 49.72% fixed carbon, 39.37% volatile matter and 10.91% ash, whereas the results of the ultimate analysis are as follows: 71.72% C, 5.06% H, 7.75% O, 1.41% N and 2.82% S.

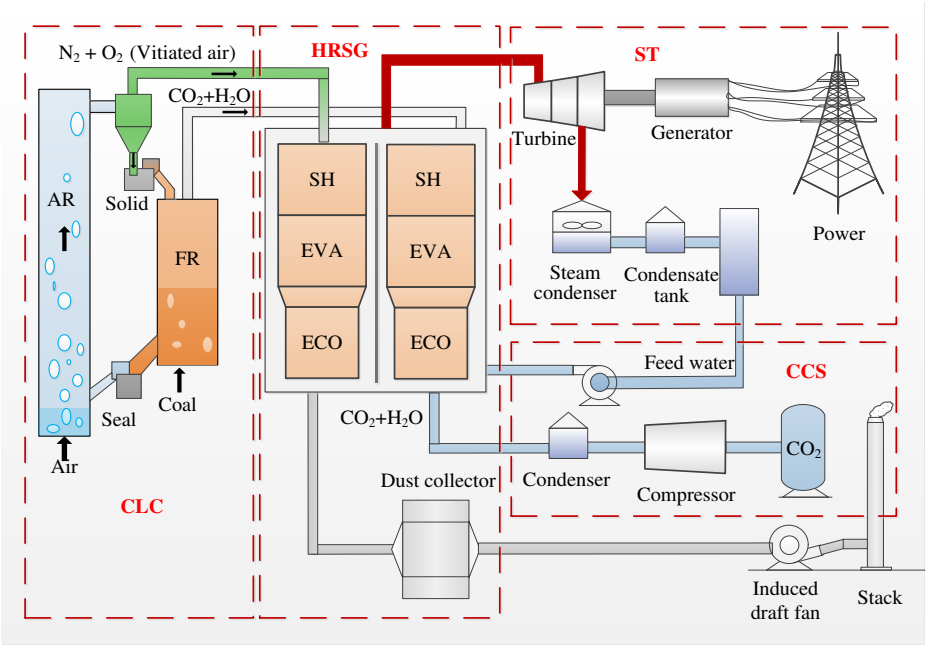

Fig. 1. Simplified scheme of CLC-power plant

Notes: air reactor (AR), fuel reactor (FR), heat recovery steam generator (HRSG), steam turbine (ST), and CO_2 capture and storage (CCS), economizers (ECO), evaporators (EVA) and superheater (SH)

Table 1. Operation conditions and design parameters of the CLC-power plant [33-37]

Units	Parameter	Value	Unit	Models	Describe
CLC	Coal	Illinois No. 6 bituminous		RYield	Yield reactor, modeling coal decomposition
	Oxygen carrier	Fe_2O_3		RGibbs	Chemical equilibria, modeling components combustion
	Reactor type	CFB		RStoic	Stoichiometric reactor, modeling in-furnace slagging process
	Coal input	63.33	kg/s		
	Temperature/ Pressure (FR)	1,173.15/0.1	K/MPa	SSplit	Substream splitter, modeling flue gas, fly ash and oxygen carrier separation
	Temperature/ Pressure (AR)	1,223.15/0.1	K/MPa		
	CO_2 recycle ratio	0.65 - 0.70		Compr	Modeling HP, IP, and LP turbines
HRSG	Economizer temperature (LT/HT)	403.15/579.15	K	Heater	Modeling gas cooling and steam heating process
	Evaporator temperature (main)	866.15	K		
	Exhaust gas temperature (AR/FR)	353.15/363.15	K		
	Air preheating temperature	550.15	K	HeatX	Modeling gas cooling and steam heating process
	Circulating CO_2 temperature	673.15	K		
	Pinch-point ΔTex_{min} in preheaters	10.00	K		
Steam turbine	Boiler feedwater temperature	579.15	K	Heater	Modeling HP heaters, LP heaters, condenser
	Live steam SH	866.15/24.2	K/MPa		
	Live steam exiting HP turbine	636.15/6.4	K/MPa	Flash2	Modeling deaerator
	Live steam RH	866.15/6.4	K/MPa		
	Number of HP/IP/LP parallel flow	2/2/5		Pump	Modeling pumps
	HP/IP/LP steam turbine isentropic efficiency	90/92/87	%		
	Steam turbine mechanical efficiency	100	%	Pump	Modeling primary air fan, secondary air fan, induced draft fan

Units	Parameter	Value	Unit	Models	Describe
CO_2 compression and liquefaction	CO_2 condensing temperature	297.15	K	HeatX	Modeling intercooling process of CO_2 compression
	Number of compression sections	5			
	Compressors isentropic efficiency	80	%		
	Compressors electric-mechanical efficiency	94	%		
	Pressure at compressors outlet	15	MPa		
	Cooling water temperature (in/out)	292.15/308.15	K	FSplit	Modeling CO_2 recycle process
	Intercooling CO_2 temperature (out)	318.15	K		

2.1 Chemical looping combustion

The heart of the power plant (CLC unit) uses a circulating fluidized bed (CFB) as the reactors (see Fig. 1). In this part, coal is injected into the FR by CO_2 flow via the conventional coal handling and feeding equipment. Lattice oxygen in the form of a metal oxide is used in the FR instead of molecular oxygen in air or high-purity oxygen, to combust the coal. FR off-gas primarily contains CO_2 and steam but also has a small percentage of particulate (flash ash), which is purged by the conventional cleaning equipment (baghouse). The reduced OC's from the FR is transported into the AR to re-oxidize it by reacting with the preheated air. The oxygen carriers are then circulated back into the FR. The clean FR off-gas and exhausted air are sent to the typical triple-pressure HRSG [34] with the common parameters (in Table 1).

2.2 HRSG unit

As shown in Fig. 2, the hot off-gases generated from the FR and AR are mainly cooled down under different pressures for the steam generation in the economizers (ECO), evaporators (EVA) and superheater (SH) / reheater (RH) [34]. These processes are considered as part 1 of the heat exchange network (HEN). The off-gases are further cooled for heating the recycled flue gas (CO_2) and air. Air is preheated to approximately 523 K in an air preheater while oxygen-depleted air is cooled from 623 K to 353 K. FR off-gas is also cooled to 363 K with the recycled gas (CO_2) preheated to 673 K. In the HRSG unit, the minimum heat exchange temperature difference between the hot stream and cold stream (ΔTex_{min}) in the heat exchangers is considered to be as 10 K [35], while some parameters (in Table 1) in the HEN are referenced in Maurizio Spinelli's work [34].

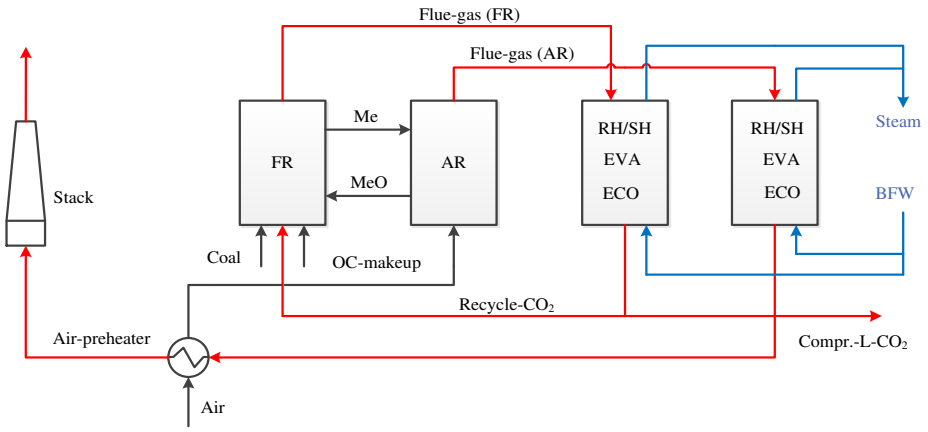

Fig. 2. HEN (Part 1) of off-gases

2.3 Steam turbine

The steam turbine is the main part for electricity generation in the CLC-power plant. In this unit, three-pressure reheat steam-water systems are employed. As shown in Fig. 3, there are a series of turbines (two high pressure (HP) turbine stages, two intermediate-pressure (IP) turbine stages, and five low-pressure (LP) turbine stages), a condenser, a series of heaters (low-pressure feed water heaters (LP FWH), high-pressure feed water heaters (HP FWH)), and a deaerator (DEA). Part of the steam can be extracted from the turbines, then used for the heating of boiler feed water (BFW), these processes are considered as part 2 of the HEN, while the deaerator is in the extraction steam of IP turbine, which is used for the heating of water and removal of oxygen. A series of heat exchangers are used to preheat BFW.

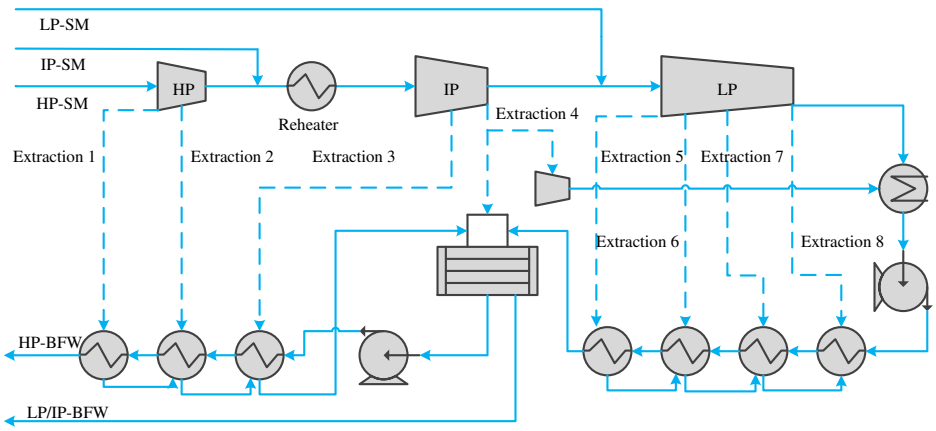

Fig. 3. Scheme of steam turbine and HEN (Part 2)

2.4 CO_2 capture and compression process

CO_2 is compressed up to 11 ~ 15 MPa for transportation and storage [36]. The traditional CO_2 separation and compression process is an energy intensive process. In this system, only CO_2 compression is required which is also energy intensive. To reduce energy consumption, the compression of CO_2 is performed in stages. In this process, the combustion products only contain CO_2 and H_2O, the merit of CLC. At each stage of the compression process, a CO_2-rich stream needs to be cooled by circulating water to reduce energy consumption. Highly concentrated CO_2 can be obtained from the FR flue gas by simple condensation without the additional energy loss. A CO_2 multistage inter-cooling compression is shown in Fig. 4. The pressure is increased up to 3 MPa using a three-stage compression with the intercooling water. Two other compression stages are added to further raise the pressure up to 15 MPa [37]. Integration of intercooling compression with steam cycle low-pressure section [38] can not only reduce energy consumption but also produce more steam for electricity generation.

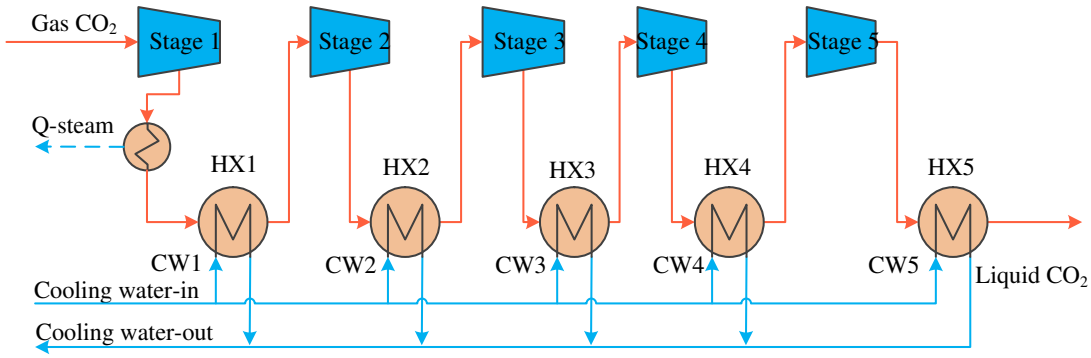

Fig. 4. Scheme of CO_2 intercooling compression

2.5 Model establishment and validation

The simulation process of CLC-power plant is established based on the main parameters of the four parts from the literatures (Table 1) and presented in Fig. S1 in the Supporting Information. Two property methods were selected for the simulation of the CLC-power plant: Peng Robinson and Boston Mathias (PR-BM) for the estimation of properties of chemical components (gas and liquid), and the STEAMNBS for water and steam [39]. CLC unit (AR and FR) is simulated by RGibbs module

[40]. Solid-gases (syngas, slag, ash and OC) separation processes are modeled by SSplit and Sep models. In the HRSG section, Heater and Heatx blocks are adopted to simulate the heat exchange and recovery. As for the ST part, Pump and Flash2 models are used to simulate the steam turbine. The detailed description of each model is summarized in the Table 1. The fundamental assumptions for the whole system are as follow:

(1) The CLC-power plant system is operated in a steady-state stable.

(2) Net power generation of the CLC-power plant system (CO_2 capture ratio is 90%) is 600 MW.

(3) AR and FR are regarded as CFBs.

(4) The material in the two reactors (AR and FR) is well mixed.

(5) The reaction between oxygen carrier and ash is not considered.

(6) Ignoring radiative heat loss of chemical looping combustion and heat transfer processes.

For validation of the CLC-power plant system, the simulation results (Table 2) of key units (CLC, steam turbine and CO_2 capture and compression) are compared with that of published literature with the same simulation conditions. CLC model is validated by using five experimental data [41, 42], in which the relative error is less than 0.5%. The simulation result of the power generation subsystem (steam turbine) is presented in Table 2, the relative error ranges from 0 to 3.5%, which shows a good agreement with the experimental data. For validation of the CO_2 capture and compression process, the energy consumption required for CO_2 compression is equal to 114 kWh/t, which is within the unit compression energy consumption range of 80 ~ 120 kWh/t (compressed between 11 MPa to 15 MPa) [43]. It can be seen that the simulated results are very close to the experimental or reference data, implying that the established models (CLC, steam turbine and CO_2 capture and compression) are reliable for the simulation of the CLC power plants system.

Table 2. Model validation

CLC								ST			
Item	input quantity of coal(g/min)	TAR (°C)	TFR (°C)	input quantity of CO_2 (LN/min)	Experimental results, CO_2 purity (%)	Simulation results, CO_2 purity (%)	Relative error (%)	Item	Literature data [44]	Simulation results	Relative error, %
1	23	970	890	5	99.65	99.97	0.32	Temperature of HP/IP/LP steam, K	866/866/534	866/866/525	1.68
2	23	970	890	3	99.63	99.94	0.31	Pressure of main steam, MPa	24.1	24.1	0
3	32	960	890	5	99.73	99.95	0.22	Boiler feed water, kg	2,003,325	2,011,883	0.43
4	46	960	890	5	99.72	99.93	0.21	Steam-to-HP, kg	2,003,325	2,011,883	0.43
5	56	970	890	5	99.45	99.92	0.47	IP-steam, kg	1,673,259	1,615,535	3.45
								LP-steam, kg	1,282,517	1,244,791	2.94
								Gross plant power, MW	642	620	3.53

3 Methodology

3.1 Energy and exergy analysis

The energy changes in the process as shown in Eqn. (1), does not supply sufficient information about the potential work lost during the process. As presented in Eqn. (1), W_{ST} represents the gross power generated by steam turbine, $W_{CO2,com}$ represents the power consumption of CO_2 compression, W_{pump} represents the work consumed in pumps, and $W_{MeO,cycle}$ represents the power consumption of oxygen carrier circulation. The net power generation efficiency (η_{net}) is defined in Eqn. (2), in which HHV_{coal} represents the higher heating value of coal used in the power plant system, and $m_{coal,in}$ represents the mass flow of coal. The gross-power generation efficiency (η_{gross}) can be calculated by Eqn. (3). Eqn. (2) to Eqn. (3) by utilizing the first laws of thermodynamics principle, and power plant exergy efficiency (Eqn. (4) (net power generation exergy efficiency) to Eqn. (5) (net power generation exergy efficiency)) used the second laws of thermodynamics principle.

$$W_{out} = W_{ST} - W_{CO_2,com} - W_{pump} - W_{MeO,cycle} \quad (1)$$

$$\eta_{net} = \frac{W_{out}}{HHV_{coal} \times m_{coal,in}} \quad (2)$$

$$\eta_{\text{gross}} = \frac{W_{ST}}{HHV_{coal} \times m_{coal,in}} \quad (3)$$

$$\eta_{\text{ex,net}} = \frac{W_{out}}{Exergy_{coal} \times m_{coal,in}} \quad (4)$$

$$\eta_{\text{ex,gross}} = \frac{W_{ST}}{Exergy_{coal} \times m_{coal,in}} \quad (5)$$

Exergy is a measure that coordinates quality with the quantity of energy. The irreversibility in a process can be accounted for a detailed exergy analysis, which uses the first and second laws of thermodynamics simultaneously. The total exergy (E) consists of physical exergy (E_{ph}) and chemical exergy (E_{ch}), which can be calculated by Eqn. (6). An environment state should be defined before the exergy calculation. The state considered is T_0 = 298 K and P_0 = 0.1 MPa, and an appropriate

environment model [45] is used in CLC-power plant. The unit enthalpies, unit entropies, unit Gibbs free energies, and unit chemical exergies of some components [45] are presented in Table S1 which shows the calculated unit E_{ch} for some components relating to the exergy of the system analyzed.

$$E = E_{ph} + E_{ch} \tag{6}$$

$$E_{i,ph} = [h(T,p) - h(T_0,p_0)] - T_0[(s(T,p) - s(T_0,p_0)] \tag{7}$$

$$E_{ph} = \sum_{i=1}^{n} x_i E_{i,ph} \tag{8}$$

$$E_{ch} = \sum_{i=1}^{k} x_k e_k^{CH} + RT_0 \sum_{i=1}^{k} x_k \ln x_k \tag{9}$$

$$E_{ch,coal} = \beta \times LHV_{coal} \tag{10}$$

$$\beta = \begin{Bmatrix} 1.0064 + 0.1519 \times (w(H)/w(C)) \\ +0.0616 \times (w(O)/w(C)) + 0.0429 \times (w(N)/w(C)) \end{Bmatrix} \tag{11}$$

The physical exergy is calculated by [14] Eqn. (7), and the physical exergy of a mixed steam can be calculated using Eqn. (8), in which x_i is the molar fraction of the gaseous mixed stream. The chemical exergy is calculated [45] using Eqn. (9). However, for the unconventional compounds (coal) [14], the chemical exergy can be calculated using Eqn. (10) and Eqn. (11) based on the ultimate analysis. where, *w(H)*, *w(C)*, *w(O)*, *w(N)* are the mass ratios of H, C, O and N in the coal, respectively.

For a steady-state process, the exergy destruction can be calculated through an exergy balance presented in Eqn. (12), in which E_{in}, E_{out} and E_D represent the input exergy, output exergy and exergy destruction of each unit respectively. The exergy destruction of the overall plant includes exergy loss in the energy conversion process and the exergy contained in material streams (such as exhaust gases, ash, and wastewater) discharged without further use, and exergy efficiency (η_{ex}) is calculated using Eqn. (13).

$$E_D = E_{in} - E_{out} \tag{12}$$

$$\eta_{ex} = \frac{E_{out}}{E_{in}} \tag{13}$$

3.2 Combined pinch and exergy analysis

Exergy is a rigorous way of analyzing energy conversion systems such as steam power plants, which can distinguish the quality of the different forms of energy. The energy level Ω is defined in Eqn. (14). In the processing system integration analysis, combined pinch and exergy analysis is beneficial for reducing the energy consumption and optimizing the heat exchanger network in steam power plants. The Exergy Composite Curve (ECC) and Exergy Grand Composite Curve (EGCC), based on two basic tools (composite curves (CC) and the grand composite curve (GCC)) in pinch analysis, is introduced in the CPEA approach [28-30]. The CPEA method used in this paper, introducing a new diagram (Ω-H diagram) as shown in Fig. S2, can represent a whole system exergy situation, including input exergy, output exergy and exergy destruction in heat transfer processes and core processes while providing targeted information. Meanwhile, major directions and promising modifications for system improvement can be identified effectively.

$$\Omega = \frac{exergy}{energy} \tag{14}$$

3.3 Economic evaluation

Techno-economic analysis starts from the estimation of the total capital investment (TCI) for the CLC-power plant following a bottom-up approach, described in the cost-estimation of the power plant [46, 47]. The hierarchy is illustrated in Fig. S3. It has four levels such as total purchased equipment cost (TPEC), total installed cost (TIC), total direct and indirect cost (TDIC), and fixed capital investment (FCI). TCI mainly depends on the TPEC, which is evaluated by industrial price data and literature sources from the economic analysis [44] and presented in Table 3. The other levels for economic estimations are calculated based on TPEC. The equipment cost is estimated using the scaling factor exponent for adapting plant size using Eqn. (15) [48]. In Eq. (12), C_0 is the known investment cost, S_0 is the capacity of the reference plant, and α is the specific factor for equipment costs which are scaled from corresponding equipment. The annual operating cost (AOC) is then analyzed. The hierarchy is shown in Fig. S4, AOCs are grouped into four categories of variable

production cost (VPC), plant overhead costs (POC), general expenses (GE) and fixed charges (FC). Those parameters are calculated using the factorial method [46]. The annual operating cost is highly dependent on the VPC, which mainly includes the cost of coal, OC, water, and carbon tax.

$$C = C_0 \times \left(\frac{S}{S_0} \right)^{\alpha} \quad (15)$$

3.3.1 Economic assumptions and criteria

Several major premises and assumptions were imposed (Table 4) in this economic feasibility analysis. The annual plant capacity factor is considered as 85% (7,446 h/y). The construction time is supposed to be one year, and the power plant lifetime is assumed to be 25 years. A study [49] reported that the lifetime of OC (LT_{OC}) for Fe_2O_3 equal to 1,315 h. The depreciation period is set to be 10 years with an 8% depreciation rate [50], and the gross income tax rate is 30% carbon tax which equals 45 \$/t CO_2 [51] and the discount ratio is 8%. The average electricity price of coal-fired power plant is 0.087 \$/kWh [52], the price of coal and industrial water are 87.0 \$/t and 0.29 \$/t - 0.43 \$/t [46, 53, 54], respectively.

Table 3. Cost estimation of power plant equipment

Parameter	Base plant* W - CCS	Estimate plant**	Unit	Scaling factor [54-58]	Base plant cost, k$	Estimate plant cost, k$
Coal handling system (coal)	224,970	228,000	kg/h	0.65	22,386	22,581
Coal and sorbent preparation and feed (coal)	224,970	228,000	kg/h	0.65	15,128	15,260
Feedwater and miscellaneous systems and equipment (BFW)	1,439,044	1,593,291	kg/h	0.6	59,843	63,613
Flue gas cleanup	173.76	178.21	kmol/h	0.6	118,843	120,660
CO_2 remove compression & drying (CO_2)	475,336	477,586	kg/h	1	50,211	50,448
Ducting and stack(coal)	224,970	228,000	kg/h	1	21,025	
Steam turbine generator and auxiliaries	2,003,325	2,184,323	kg/h	0.6	116,957	123,187
Cooling water system	224,970	228,000	kg/h	0.6	20,725	20,892
Ash and spent sorbent recovery and handling (ash)	22,099	22,287	kg/h	0.67	6,738	6,776

Notes: * NETL/DOE. ** the flow rates are calculated by the aspen plus.

Table 4. Economic assumptions and estimation of annual operating cost

Parameters	Values	Annual operating cost			
Financing	100% owned capital	**Variable production cost (VPC)**		**General expenses (GE)**	
Plant availability	7,446 h/y (~ 85%)	Raw material	-	Administrative costs	0.15%TCI
Plant depreciation period	10 years	Operating labor (OL)	0.5%TCI	**Plant overhead costs (POC)**	
Construction period	1 year	Operating supervision (OS)	15%OL	60%*(OS+OL+MR)	
Plant life	25 years	Maintenance and repairs (MR)	2%DPE	**Fixed charges (FC)**	
Income tax rate	30%	Operating supplies	155%MR	Financing	5%TCI
Electricity cost	0.087 $/kWh	Laboratories charges	15%OL	Local taxes	2%FCI
Carbon tax	45 $/t CO_2	VPC	115%FCI	Property insurance	1%FCI
Discount rate	8%	**Annual operating cost = VPC+GE+FC+POC**			
Coal price (Illinois No. 6 bituminous)	87.0 $/t				
OC lifetime	1315 h				
OC price	293 $/t				
Industrial water price	0.362 $/t				

3.3.2 Total capital investment

Most equipment components in the CLC power plants are conventional, such as the coal preparation and handling system, gas cleaning system, steam generation and steam turbine generator system, cooling water system, ash and spent sorbent handling systems, HRSG, ducting and stack, and CO_2 compression and drying, etc. Their costs can be estimated by scaling from equivalent equipment costs of the reference plant [44]. As for other equipment components in the CLC power plant, the FR, AR, and their associated subsystems are in the development stage. Their costs must be estimated by approximate sizing of the equipment (analogical) and application of general cost correlations.

As mentioned above, the factorial method is used to estimate the capital cost of power plants. For conventional units, the cost of capital investment is the sum of FCI and working capital (WC = 15% FCI). The FCI consists of TDIC and project contingency (PC = 20% TDIC), in which TDIC is composed of TIC and indirect costs (IC = 89% TPEC). TIC is composed of purchased equipment installation, instrumentation and control, piping, electrical system, buildings, yard improvements, service facilities and land, etc. The sum of all these factors can be estimated to be equal to 198% [59] of TPEC. All the estimated equipment costs (Table 3) were converted to the year 2018 (CEPCI, Table S2) calculated by using CEPCI in Eqn. (16). The cost estimation of combustor equipment in the CLC-power plant is different from conventional combustor units. For the CLC combustor, the FR needs to be insulated. In contrast to the corresponding walls of a traditional combustor, these insulated walls will not be involved in the transfer of heat to the steam. Moreover, the cost of insulation for the cyclones of FR and ducts leading material to FR are added [60]. Therefore, TCI of the CLC part is estimated by the equipment of the CLC power plant [61]. The present cost of the CLC part is calculated by using Eqn. (16).

$$Cost_{present} = Cost_{reference} \times \frac{Index_{in\ present\ year}}{Index_{in\ reference\ year}} \quad (16)$$

3.3.3 Annual operating cost

In Table 4, the expenditures affecting the AOC of the power plant based on average percentages are listed which includes the variable production cost (VPC), fixed charges (FC), plant overhead costs (POC) and general expenses (GE). The VPC is highly dependent on the cost of raw materials which mainly counts for coal, cooling water and the OC make-up expenditures. The annual cost of the OC make-up is defined in Eqn. (17). FC, POC and GE are calculated and presented in Table 4. The detailed cost date of raw material is presented in Table 4.

$$Cost_{makeup} = Cost_{OC} \times \frac{M_{OC}}{LT_{OC}} \tag{17}$$

3.3.4 Cost of electricity

With the application of basic assumptions of the economy, once the TCI and AOC are estimated, economic criteria such as cost of electricity (COE), capital recovery factor (CRF), the annual average of return on investment (ROI) and net present value (NPV) are obtained from the following equations (Eqns.18-21). The NPV is the sum of the total net cash flows after the discounting during the plant lifetime [48, 62], and it is calculated using Eqn. (18) where i is the discount rate, C_t refers to the net cash flow over t years. COE is an economic index for comparing the different power generation technologies, which is calculated using Eqn. (19). TPC is the total plant cost, and AOC refers to the total variable cost. CRF refers to the capital recovery factor which can be obtained using Eqn. (20), which is a function of the discount rate (i) and the expected plant lifetime (y). ROI, one of the commonly used economic criteria to evaluate the feasibility of a project, is calculated using Eqn. (21), where P is the profit of the power plant, TR is the tax rate.

$$NPV = \sum_{t=1}^{y} \frac{C_t}{(1+i)^t} \tag{18}$$

$$COE = \frac{TCI \times CRF + AOC}{7446 \times W_{net}} \tag{19}$$

$$CRF = \frac{i}{1-(1+i)^{-y}} \tag{20}$$

$$ROI = \frac{P}{TPC \times CRF + TVC} \tag{21}$$

3.4 Technical evaluation

The carbon capture ratio [44] is defined as the amount of carbon captured relative to the total carbon input, represented by Eqn. (22). The coal consumption [44] and CO_2 emission [44] of a power plant, evaluating the economic and environmental performance of a power plant, are shown in Eqn. (23) and Eqn. (24), respectively. The energy consumption [44] of CO_2 capture, which means energy consumption caused by CO_2 capture process, is defined by Eqn. (25).

$$Carbon\ capture\ ratio,\ \% = \frac{Carbon\ captured}{Total\ carbon\ input} \tag{22}$$

$$Coal\ consumption,\ g/kWh = \frac{Total\ coal\ input}{Net\ power\ generated} \tag{23}$$

$$CO_2\ emission,\ g/kWh = \frac{CO_2\ emissions}{Net\ power\ generated} \tag{24}$$

$$Energy\ consumption\ of\ CO_2\ capture,\ kW/t = \frac{Energy\ consumption}{CO_2\ captured} \tag{25}$$

4 Results and Discussion

4.1 Effects of key parameters on performance

Generally, CLC of solid fuels was conducted under atmospheric pressure [63-65] due to the requirements of massive additional energy penalty for OC circulation and expensive equipment investment for high-pressure CLC processes. Therefore, in this section, the temperature during combustion, the mass ratio of oxygen carrier to coal (OC/C = R), and recycle ratio of carrier gas is tested which are the vital factors that affect the exergy efficiency of CLC ($\eta_{ex,CLC}$), $\eta_{ex,net}$ and η_{net}.

4.1.1 The mass ratio of oxygen carrier to coal

The main cornerstone in CLC is the oxygen carrier. The amount of OC circulated from the AR

must provide enough oxygen for the complete coal combustion, as well as enough heat for the CLC's autothermal operation [66]. Therefore, the value of R not only affects the composition of the FR output stream but also can affect the temperature of the fuel reactor (TFR). In Fig. 5, CO_2 recycle ratio (0.65) and temperature of the air reactor (TAR) (1,223 K) are fixed. With the increase in R, the mole fraction of CO_2 increases from 73 to 78% (wet basis), while the mole fraction of CO, H_2, CH_4 decreases nearly to zero, as shown in Fig. 5 (a). When the value of R exceeds 55, the CO gas is converted to CO_2 completely (Fig. 5 (b)). In the case of CLC's autothermal operation condition, different values of R correspond to different TFRs (Fig. 5 (c)). As the value of R increases, the ΔT of two reactors decreases. For the specific implementation in CLC, two factors should be considered: one is easy enrichment and separation of CO_2 from FR, the other is autothermal operation of CLC. Combining these two factors, the value of R should be more than 55.

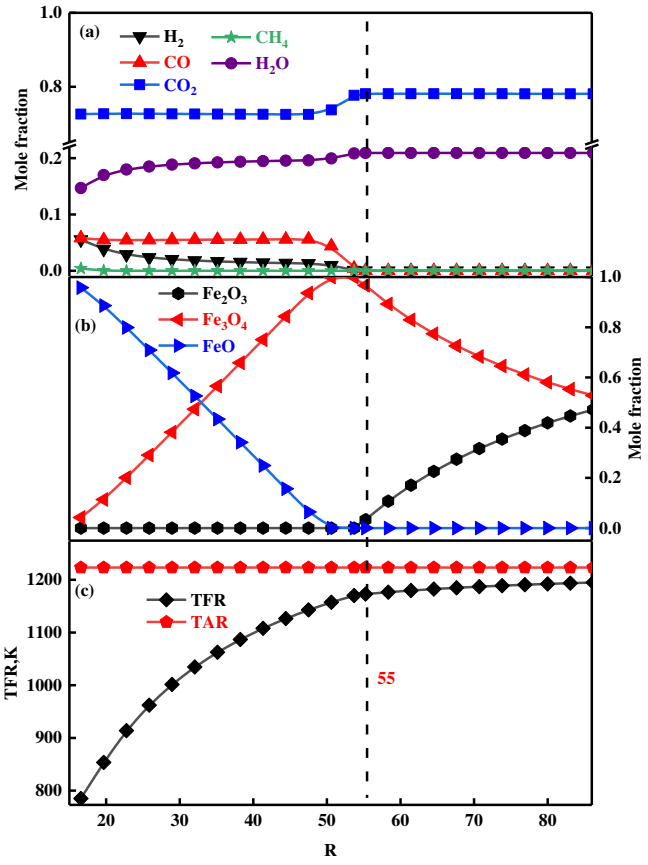

Fig. 5. The effect of R on the performance of CLC about flue gas (a), OC (b) composition in FR and TFR (c)

4.1.2 Temperature difference of air reactor and fuel reactor

Under CLC's autothermal operation, TFR is determined by the value of R and TAR. The mathematical relationship among them is presented in Fig. S5. Fig. 6 (a) shows the effect of TFR on the energy efficiency (η_{gross} and η_{net}) of a CLC-power plant. Combining Fig. 5 and Fig. 6 (a) shows that, if the value of TFR is less than 1,157 K, a decrease in the CO_2 purity is obtained with the further reduction of the OC into FeO or Fe. However, if the value of TFR is greater than 1,157 K, in order to maintain autothermal operation state, excess Fe_2O_3 should exist in the FR as a heat carrier. More OC will require more power consumption for the OC fluidization which will reduce $\eta_{ex,CLC}$ and η_{net}. There is a tradeoff between ΔT and η_{net}, which is determined by the amount of OC. Therefore, based on the judgment of efficiency and R, the optimal ΔT (66 K) is selected.

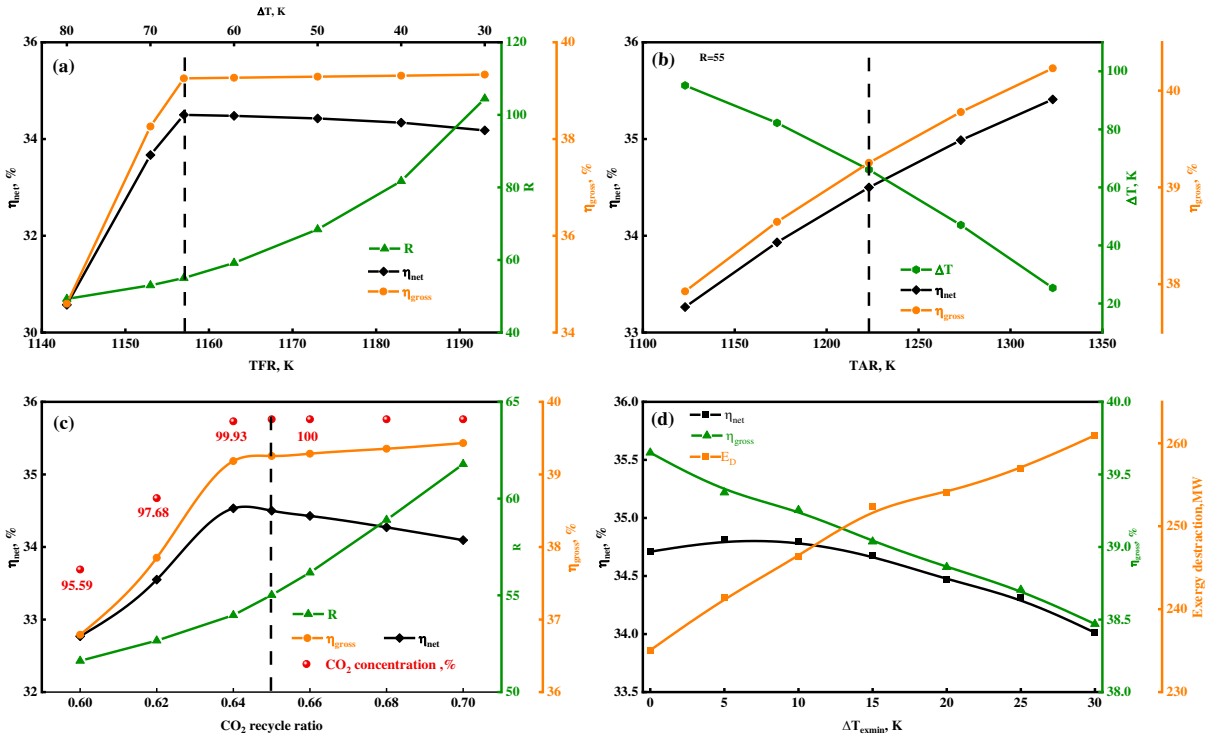

Fig. 6. Effect of different factors (a-ΔT and TFR; b-TAR; c- CO_2 recycle ratio; d-ΔTexmin) on power generation efficiency, R, ΔT, or HEN exergy destruction

4.1.3 Temperature of air reactor

Referring to previous reports [40, 67, 68], CLC of solid fuels is performed in CFBs within the

CFB temperature range 1,073 K - 1,273 K. The maximum temperature in the reactors is between is 1,273 K - 1,473 K [69, 70]. TAR and TFR are determined to describe the properties of the OC (Fe_2O_3), such as particle deactivation from fusion, sintering and melting. Previous fluidized bed studies determined 1,323 K as the upper operating limit, which would present the agglomeration problems for Fe_2O_3 (iron ore/ilmenite). In the previous section, autothermal operation cases were studied, however, this section examines the effects of different TAR within the temperature 1,123 K - 1,323 K on CLC-power plant energy efficiency and ΔT with a fixed amount of oxygen carrier (R = 55). The trend is shown in Fig. 6 (b), showing that the energy efficiency of the power plant increases but ΔT of the reactors decreases with an increase in TAR. To avoid OC fusion, sintering and melting, an appropriate ΔT (66 K) is favorable for a high heat transfer rate and appropriate OC circulation ratio. Eventually, TAR equal to 1,223 K is selected.

4.1.4 CO_2 recycle ratio

In CLC power plants, recycled CO_2 can be used as the carrier gas for OC circulation and as a heat energy carrier to maintain the combustion temperature inside the CLC unit. Different CO_2 recycle ratio can lead to different fluidization velocity, which effects the amount of OC, consequently effecting the equilibrium of reaction and heat balance of CLC. The flue gas recycle ratio is generally between 0.6 - 0.7 [34, 58, 71] in a CFB. The CO_2 recycle rate for FR affects the total performance of the CLC-power plant regarding both energy efficiency and CO_2 capture. From the previous sections, the following conditions are selected (TAR = 1,223 K; TFR = 1,157 K). The effect of different CO_2 recycle ratios on R and power efficiency is presented in Fig. 6(c). With an increase in CO_2 recycle ratio, the η_{gross} sharply increases at the beginning then tends to slow down due to the different consumption of OC. While the η_{net} increases sharply at the beginning, it then decreases due to an increase in power consumption, which is caused by the increase in energy required for CO_2 compression and OC fluidization. The maximum concentration (~ 100%) of CO_2 can be achieved when CO_2 recycle ratio is more than 0.65. However, the higher CO_2 recycle ratio causes the

consumption of more OC. Therefore, the optimal recycle rate of CO_2 is approximated to be 0.65.

4.2 Combined pinch and exergy analysis

This method quantifies the total, avoidable and unavoidable exergy loss for the processes (or equipment), which presents the potential improvement for the HEN heat recovery from Part 1 and Part 2. Generally, according to the HEN empirical design, the range of ΔTex_{min} is between 0 ~ 30 K, with 5 K being taken as the step length to investigate its influence on the HEN exergy efficiency and power generation efficiency. It can be seen that ΔTex_{min} of 10 K (Fig. 6(d)) can achieve the maximum power generation efficiency (34.80%) with the HEN exergy efficiency of 82.15% (part 1) and 87.98 % (part 2). The HEN model (divided into three parts: CLC and heat recovery steam generation, Steam turbine and CO_2 capture and compression) of the three cases is presented in Fig. S6 (initial case), S7 (optimal case) and S8 (limit case), alongside the detailed parameters of hot and cold streams of the two cases shown in Table S3 and Table S4. As the CPEA method introduced in this study, Ω versus enthalpy as axes, the shaded area between hot and cold exergy composite curves (Fig. 7) indicates the initial, optimal, and minimal exergy loss in the heat exchange process. At the optimal case (ΔTex_{min} = 10 K), the blue area indicates the applicable exergy. At the limiting case (ΔTex_{min} = 0 K), the yellow area represents the minimum exergy destruction (unavoidable) that could be achieved theoretically. In Fig. 7 (c) and 7 (d), the exergy efficiency of part 1 and part 2 are 82.15% and 87.98%, which means 217.01 MW and 29.31 MW exergy destruction are caused, respectively. However, the points where both the curves touch each other in Fig. 7 (e) and 7 (f) indicate that the maximum exergy efficiencies that could be achieved in the HEN are 82.71% and 90.52% for part 1 and part 2, respectively. ΔTex_{min} has a noticeable effect on the HEN, mainly impacting the amount of energy and energy grade involved in the Hot or Cold stream (especially for extraction steam of steam turbine and LP, IP and HP steam), thus determining the power output of the steam turbine from steam generated (from the hot stream) as shown in Fig. 7 (changes of CLC and heat recovery steam generation, steam turbine and CO_2 capture and compression part in heat exchanger network were shown in Fig.S6-S8, in which the heat

duty (amount of energy to be transferred) of the heat exchanger are presented in detail). This limiting value of the exergy destruction can be considered as the technically unavoidable irreversibility of the HEN. In this regard, the exergy destruction of the two parts is 207.72 MW and 27.33 MW, respectively. It can be concluded that for the optimal case (ΔTex_{min} = 10 K), there is a recoverable 11.27 MW exergy as compared to the limit case (ΔTex_{min} = 0 K).

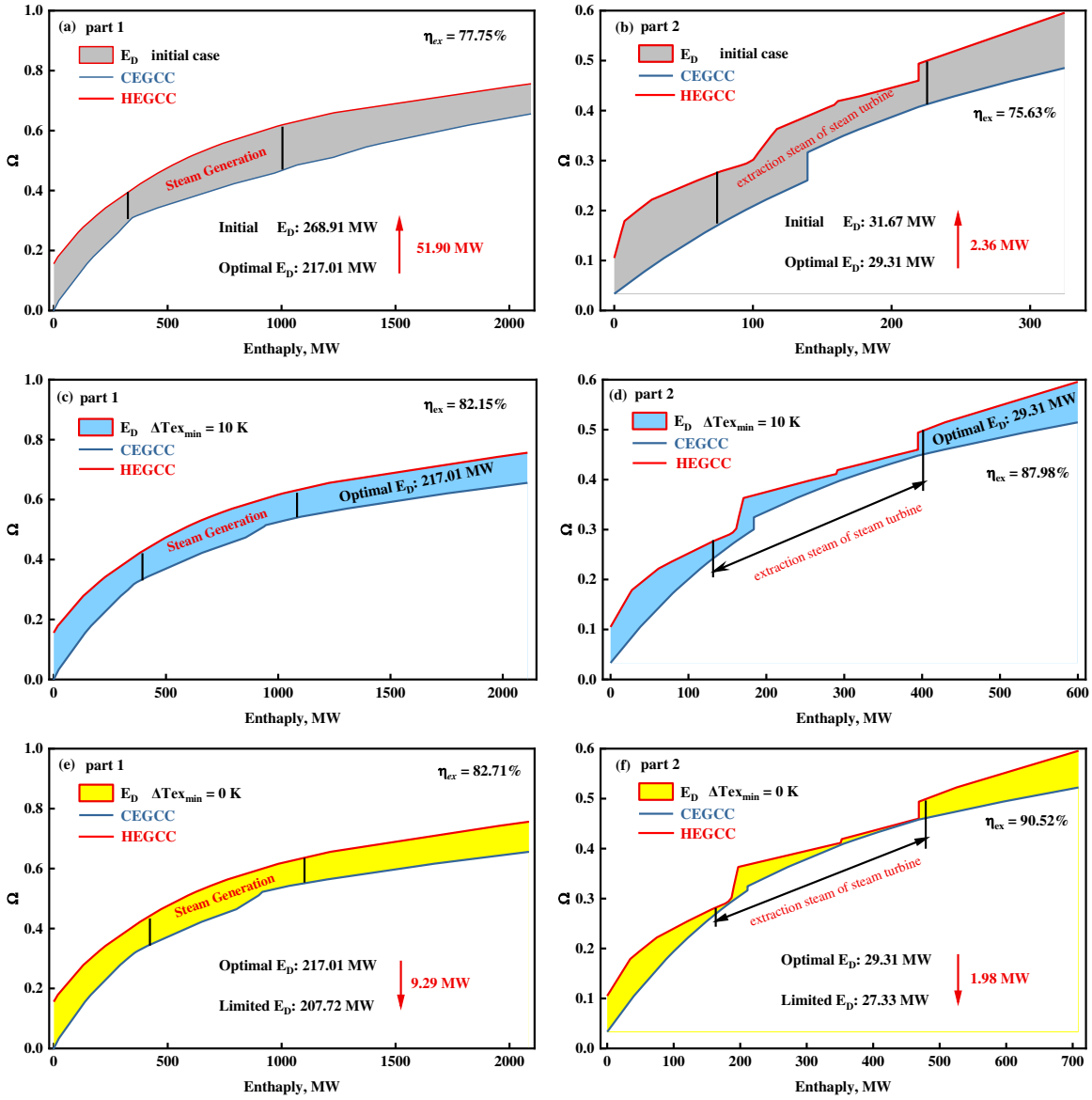

Fig. 7. The CPEA analysis results of composite curve of the whole system

Notes: Hot Exergy Grand Composite Curve (HEGCC), Cold Exergy Grand Composite Curve (CEGCC)

4.3 Effect of R and TAR on energy efficiency and COE

Based on the optimal HEN model, the results obtained from the optimization of $\eta_{ex,CLC}$ and η_{net} are shown in Fig. 8 (a) and Fig. 8 (b), which also shows the effect of R and TAR. In CLC (autothermal) unit, TFR depends on the amount of regenerated OC from the AR and OC temperature exiting the AR. In this case, we make the alternate assumption that the OC temperature entering the FR is the same as the temperature exiting the AR. In Fig. 8 (a), an increase in $\eta_{ex,CLC}$ favors higher R and higher R favors complete combustion. However, increasing the amount of OC has little effect on the CLC exergy efficiency when the value of R exceeds 55. In Fig. 8 (b), it is shown that η_{net} favors higher TAR. At a higher flue gas temperature, more steam can be produced hence more electricity is generated. For those reasons, it is suitable to work with higher OC inlet temperature (1,223 K ~ 1,273 K) and an appropriate amount of R (~ 55) to achieve higher $\eta_{ex,CLC}$ (71.72%) and η_{net} (34.84%). Fig. 9 (c) shows the different results of COE as the functions of both R and TAR. At R ratio of 55, the coal-contained-carbon is completely converted to CO_2, resulting in complete combustion. An increase in TAR, results in a decrease in COE, however, the COE increases with an increase in the amount of OC. As analyzed above (without considering carbon tax), at TAR = 1,223 K and R = 55, the value of COE is equal to 0.104 $/kWh.

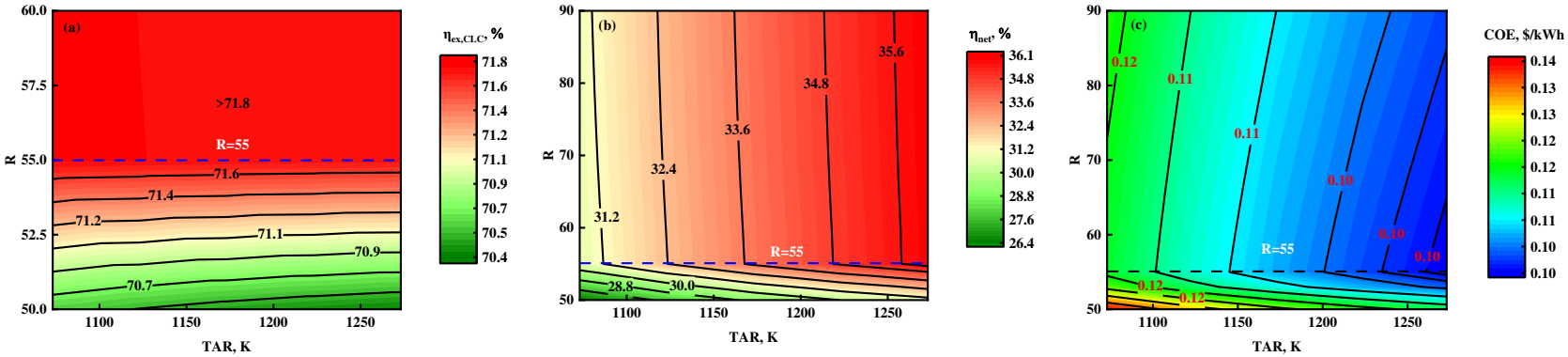

Fig. 8. Effect of R and TAR on $\eta_{ex,CLC}$ (a) and CLC-power plant η_{net} (b) and on COE (c)

4.4 Economic performance

An economic assessment was conducted to compare the novel combustion technology (CLC) power plant with the traditional coal-fired power plant. In order to compare, from an economic perspective, several conventional economic indicators (i.e., COE, ROI, NPV) have been calculated. Considering the variation of some economic parameters that are likely to change in the future, a sensitivity analysis is also shown in this section.

4.4.1 Impact of feedstock cost

Fig. 9 (a) describes the effect of the material cost of OC on ROI, NPV and COE. Compared to the current price of OC (293.04 $/t), the changes in COE, ROI and NPV are noticeable, with a decrease in ROI to 7.39% (39.41% change) and a negative NPV (49.90% change) as the OC price increases from 59 to 638 $/t. Moreover, the value of COE increases to 0.109 $/kWh (9.09% change). The main reason is the expensive price of OC and the relatively shorter LT_{OC} (High OC requirement). Fig. 9 (b) illustrates that with an increase in LT_{OC}, the COE decreases sharply then tends to plateau. However, the value of ROI and NPV rapidly increases, then plateaus. Regarding the influence of LT_{OC} on COE, NPV and ROI, they are kept stable when LT_{OC} is greater than 1,315 h (base LT_{OC}). The results presented in Fig. 9 (a) and Fig. 9 (b) suggest that the OC with a long lifetime (highly stable properties) and cheap price is pivotal for the economic performance of the CLC-power plant.

The impacts of the coal price on ROI, NPV and COE are illustrated in Fig. 9 (c). The relation between coal price and both NPV and COE is linear, as expected. The COE increases sharply however NPV decreases dramatically as the coal price goes up to 101.5 $/t from 29.0 $/t, resulting in a 32.51% increase in COE (0.084 $/t to 0.110 $/kWh). With the increase of coal price, the ROI decreases sharply as well. Those results imply that the feasibility of the power plant is affected by the price of coal.

4.4.2 Impact of run time

Fig. 9 (d) shows the effect of annual operation hours on COE, ROI and NPV. As the run time increases, the COE decreases sharply which indicates more favorable conditions, while NPV and ROI values are remarkably increased. In general, the long run time represents the high output of electricity and lower COE. A relatively low COE of 0.104 $/kWh is obtained, and a high ROI (15.60%) at an operating rate of 85% (7,446 h) is obtained. However, when the power plant operating time is reduced (6,000 h), the COE (0.119 $/kWh) is almost equal to the traditional power plant (W-CCS) at a higher operating time (7,446 h). So, compared to the traditional coal-fired power plant (W-CCS), the CLC-power plant has a significant advantage in COE.

4.4.3 Impact of electricity prices

Revenues for electricity sales are significant, especially for the economic viability of the power plant. As shown in Fig. 9 (e), it is seen that when E-prices are higher than 0.100 $/kWh and lower than 0.128 $/kWh, the NPV will exceed zero at a discount rate of 0.06 and 0.12, respectively. With an increase in the discount rate, the E-price needs to remain high to keep NPV exceeding zero. Additionally, the feed-in tariff rate of coal power plants (without CCS) is currently 0.087 $/kWh. Hence, the CLC power plant is clearly unprofitable when the discount rate is 0.08.

4.4.4 Impact of carbon allowance price

The reference base price of carbon price in China is 35 $/t - 50 $/t [51], in this study, we choose 45 $/t carbon tax in CLC-power plant analysis. Considering the rapid rise in the carbon price has already started to materialize, many developing countries need to adopt the carbon price and emission trading system making to match the policy for CO_2 reduction to protect the environment. Based on Fig. 11 (d) and Fig. 11 (e), it is known that, at the current E-price of feed-in tariff (0.087 $/kWh), the CLC-power plant has little advantage in the ROI and NPV. While when the E-price of the feed-in tariff is in the range of 0.100 $/kWh - 0.128 $/kWh, the CLC power plant can be profitable. More importantly, if the carbon tax is to be implemented in the future, the CLC-power plant with low CO_2

emissions will present greater advantages economically. Therefore, in Fig. 9 (f), with the carbon price is above 33.20 \$/t CO_2, it would have a positive NPV in the CLC-power plant with the current selling price of electricity (0.087 \$/kWh). Moreover, the CLC-power plant has a higher ROI (37.99%), representing the feasibility of the power plant. Therefore, a carbon trading policy might be a good option to reduce the CO_2 emission from coal power plants. When carbon trading is implemented, the economic feasibility of the 600 MW CLC-power plant (with CO_2 capture) might be viable for commercialization.

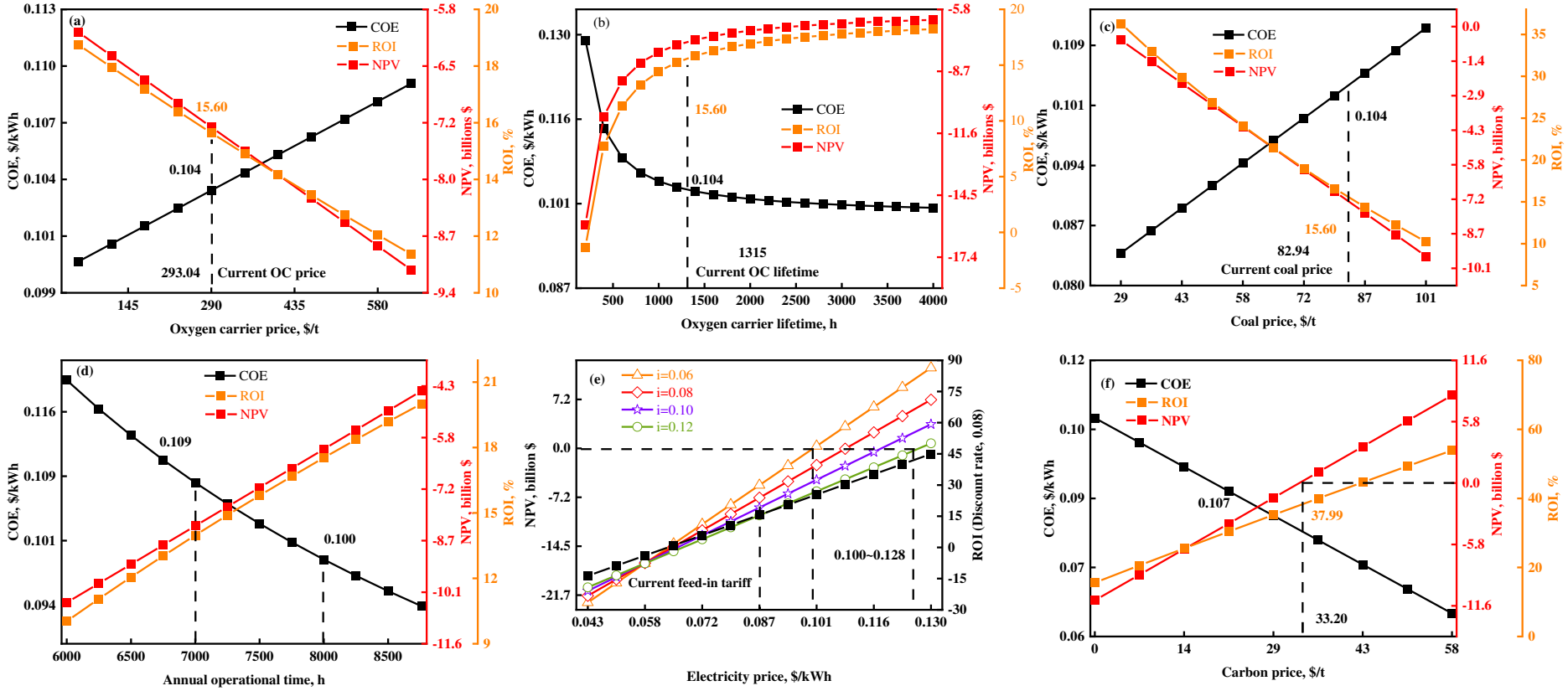

Fig. 9. Sensitivity analysis (a-oxygen carrier price; b-oxygen carrier lifetime; c-coal price; d-annual operational; e-electricity price; f-carbon price) of economic indicators (COE, ROI, NPV)

4.4.5 Sensitivity analysis on COE

In this section, the sensitivity analysis is implemented to confirm the parameters that have a remarkable impact on COE. Seven typical parameters have been selected for the sensitivity analysis over the expected range of parameters variation as shown in Table S5. Fig. 10 shows the effects of seven typical parameters on COE (0.104$/kWh) for a 600 MW CLC power plant, and the shows the COE (0.143$/kWh) of MEA-based power plant. The TCI has a noticeable impact on COE, around 18.11% variation can be observed when the TCI increases or drops by 30%. Followed by the 8.66% change that is caused by the 30% coal price variation. These results show that reducing the TCI and coal price are the most effective ways to strengthen the economic performance. More importantly, looking further at Fig. 10, it can be found that the COE of CLC (0.088 $/kWh ~ 0.127 $/kWh) are still lower than that of the MEA-based power plants (0.143$/kWh) even under negative variation (30%) of main variables, indicating the strong economic feasibility of CLC power plants.

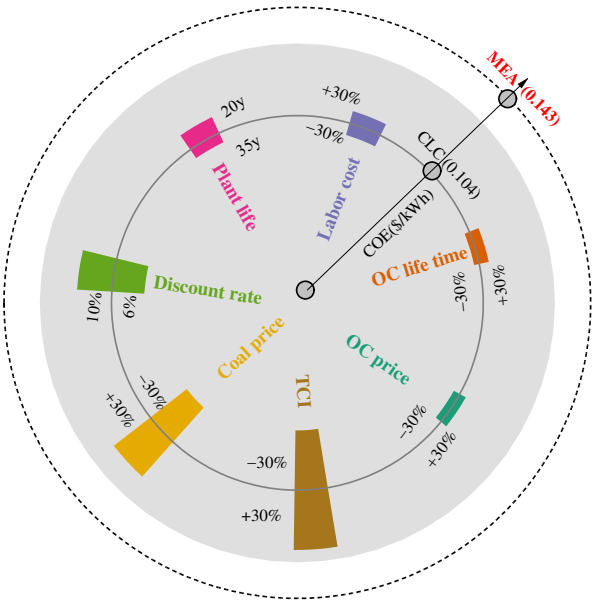

Fig. 10. Effects of some key parameters on COE

4.5 Exergy analysis and exergy distribution of CLC power plant

CLC power plant is similar to the base power plant in reference, however, the combustion unit is the main difference that distinguishes both the technologies. CLC power plants with CO_2 capture reduces the energy penalty due to the flue gas being highly concentrated with CO_2 (~ 100%). In order to get a detailed distribution of exergy, the CLC power plant is divided into four different units: combustor (CLC), HRSG, ST and CO_2 capture, and compressed. Though the differences between the CLC power plant and the base plant are only the combustion section and CO_2 capture part, the exergy distribution and dissipation of the CLC power plant are different for the base power plant. Hence, an exergy distribution analysis is conducted for the power plant in detail as shown in Fig. 11.

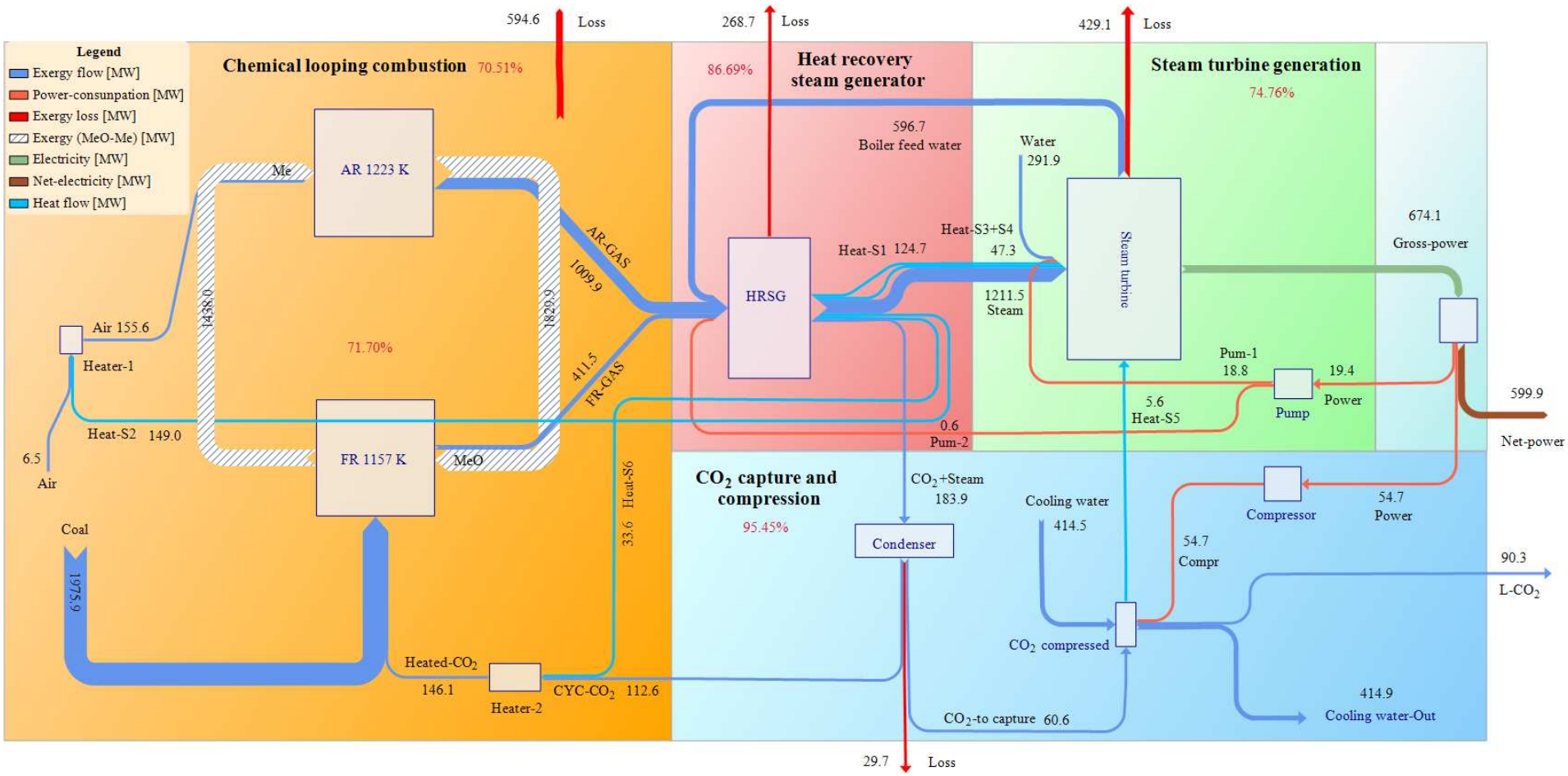

Fig. 11. Grassmann diagram (exergy distribution) of the CLC-power plant

Based on the simulation results and exergy calculation methods introduced, the exergy distribution in each unit is presented in Fig. 11. The exergy efficiency of each unit, as well as the whole power plant, can be calculated by Eqn. (4, 5, 13). The exergy efficiency of each unit (CLC, HRSG, ST, CCS) is 70.51%, 86.69%, 74.76%, 95.46%, respectively, while the exergy efficiency of the CLC-power plant is 30.27%.

In the CLC unit, coal is combusted in the FR with the OC and the exergy (E_{ch}) of coal (1,975.9 MW) is converted to exergy (E_{ph} and E_{ch}) of the flue gas, as well as E_{ph} of the reduced OC. The reduced OC is then oxidized by the pre-heated air. Meanwhile, a large amount of exergy loss (594.6 MW) takes place in the CLC unit. In this study, the combustion exergy efficiency of the CLC is 71.70%, which is similar to previous studies (74.7% - 83.25%) [72, 73], due to the different nature of the fuels, demonstrating the reliability and accuracy of the proposed model. However, the combustion exergy efficiency of CLC is higher than that of traditional combustion (50.0% - 67.6%) [8, 39, 45, 74]. This is one reason why CLC power generation efficiency is higher than traditional combustion power generation efficiency with the same CO_2 capture ratio. Another reason for the higher power generation efficiency of the CLC power plant is that the in-suit CO_2 removal property of CLC. As Grassmann diagram shows, the exergy efficiency of the CO_2 capture and compression section is 95.45%, which is higher than the traditional CO_2 capture method (~ 40.7%) [39].

4.6 Performance comparison

Table 5 presents the performance comparison between the CLC-power plant and traditional ultra-supercritical power plant w/o CCS in terms of economic, environmental, and technical indicators mentioned above. By optimizing the heat exchange network, COE, CO_2 emissions, energy consumption of CO_2 capture and coal consumption decreased by 0.009 $/kWh, 6.76 g/kWh, 25.41 kW/t and 22.6 g/kWh, respectively. With the same CO_2 capture ratio of 90%, the net generating efficiency of the CLC-power plant (optimal case) is 2.4% higher than that of the

traditional ultra-supercritical power plant with CCS (MEA-based power plant), leading to a lower COE at 0.104 $/kWh compared to 0.143 $/kWh for the MEA-based power plant. Moreover, coal combustion of the CLC-power plant is 381 g/kWh while that of the MEA-based power plant is 408 g/kWh, resulting in lower CO_2 emission of CLC-power plant at 87.7 g/kWh in comparison with that of MEA-based power plant at 97.1 g/kWh [44]. With respect to the energy consumption of CO_2 capture (only the process of CO_2 separation and compression are considered), the CLC-power plant (73.2 kW/t) is more energy-efficient than the MEA-based power plant (107.5 kWh/t). The addition of CO_2 capture and compression of the two cases result in an efficiency penalty of 5.1% absolute percent in the CLC-power plant and 8.2% absolute percent in the MEA-based power plant. Besides, the CLC-power plant can save 39.1% initial capital cost based on that of the MEA-based power plant (0.067 $/kWh). Those results demonstrate that the CLC-power plant seems to be more efficient, cost-effective, environmentally benign in comparison to the MEA-based power plant.

Table 5. Performance comparison between CLC-power plant and traditional ultra-supercritical power plant

Indicator	CLC-power plant (Before optimization, initial case)	CLC-power plant (After optimization, limit case, ΔTex_{min} = 0 K)	CLC-power plant (After optimization, optimal case, ΔTex_{min} = 10 K)	Traditional ultra-supercritical power plant [44]	
CCS/Non-CCS	CCS	CCS	CCS	CCS	Non-CCS
Capital cost, $/kWh	0.044	0.039	0.041	0.067	0.036
COE, $/kWh	0.112	0.103	0.104	0.143	0.087
Net generating efficiency, %	32.90	35.23	34.80	32.40	40.70
Gross generating efficiency, %	36.70	39.66	39.10	37.80	42.90
Combustion exergy efficiency, %	71.70	71.70	71.70	67.60	67.60
Net exergy generating efficiency, %	32.25	34.48	34.05	31.71	39.83
Gross exergy generating efficiency, %	35.91	38.81	38.26	36.99	41.98
CO_2 emissions, g/kWh	94.46	86.97	87.70	97.10	773.37
Energy consumption of CO_2 capture, kWh/t	73.21	73.21	73.21	107.58	0
Efficiency penalty of CO_2 capture, %	5.14	5.14	5.14	8.20	0
Coal consumption, g/kWh	409.2	376.8	381.0	408.0	325.8

5 Conclusions

From the above analysis and evaluation, the CLC power plant presents a low carbon, economic and efficient power generation technology which can solve the issues related to the CO_2 emission and energy utilization simultaneously in coal power generation processes. It is possible to make the following conclusions:

(1) The key operation parameters and conditions of CLC of coal were tested and optimized. The optimal values for the temperature of the air reactor (1,223 K), the temperature of the fuel reactor (1,157 K), the mass ratio of oxygen carrier to coal (55) and CO_2 recycle ratio (0.65) have been identified. These values are expected to give optimum results for complete combustion, obtaining approximately 100% concentrated CO_2 stream at a high CLC exergy efficiency (71.70%).

(2) The heat exchange network model is optimized by using combined pinch and exergy analysis, followed by obtaining the exergy distribution of the entire plant. In comparison to the optimal heat exchange network, the exergy efficiency of the limited heat exchange network increased by 0.56% (Part 1) and 2.54% (Part 2). The exergy destruction of each unit was estimated, in which the chemical looping combustion unit has the largest exergy destruction (~ 595 MW), and the steam turbine unit has 429 MW exergy destruction. Exergy distribution analysis shows that the exergy efficiency of the subsystems is 70.51% (CLC), 74.76% (ST), 86.69% (HRSG) and 95.46% (CC), respectively. The net exergy efficiency of the CLC power plant (34.05%) improved by 1.80% after HEN optimization.

(3) With the same CO_2 capture ratio of 90%, the chemical looping combustion power plant has provided a lower cost of electricity at 0.104 $/kWh and coal consumption at 381 g/kWh as compared to those of 0.143 $/kWh and 408 g/kWh in the MEA-based power plant. Even under negative variation (30%) of main variables, CLC power plant still has advantages in COE (0.088 $/kWh ~ 0.127 $/kWh) compared to the MEA-based power plant (0.143 $/kWh). Carbon price (>

33.20 \$/t-CO_2) is necessary for the future carbon market for the chemical looping combustion power plant to be profitable.

Acknowledgements

The authors gratefully acknowledge the financial support from the National Key R&D Program of China (2018YFB0605404), the National Natural Science Foundation of China (U1810125, 51776133), and the Key R&D Program of Shanxi Province (201903D121031).

Nomenclature

Abbreviations

AR	air reactor
AOC	annual operating cost
BFW	boiler feed water
CLC	chemical looping combustion
CC	composite curves
COE	cost of electricity
CO_2	carbon dioxide
CFB	circulating fluidized bed
CRF	capital recovery factor
CCS	CO_2 capture and storage
CPEA	combining pinch and exergy analysis
DEA	deaerator
ECO	economizers
ECC	Exergy Composite Curve
EGCC	Exergy Grand Composite Curve
EVA	evaporators
FR	fuel reactor
FWH	feed water heaters
FCI	fixed capital investment
FC	fixed charges
GCC	grand composite curve
GE	general expenses

HEN	heat exchange network
HRSG	heat recovery steam generator
HHV	high heating value
HP	high pressure
IP	intermediate-pressure
LP	low-pressure
MEA	monoethanolamine
NPV	net present value
OC	oxygen carrier
POC	plant overhead costs
RH	reheater
ROI	annual average of return on investment
ST	steam turbine
SH	superheater
TRL	technical readiness level
TCI	total capital investment
TPEC	total purchased equipment cost
TIC	total installed cost
TDIC	total direct and indirect cost
TFR	temperature of fuel reactor
TAR	temperature of air reactor
VPC	variable production cost
WGS	water gas shift

Reference:

[1] BP. Technology Outlook. 2018; https://www.bp.com/technologyoutlook2018. [accessed July, 30 2019].

[2] Zeng L, Kathe MV, Chung EY, Fan L-S. Some remarks on direct solid fuel combustion using chemical looping processes. Curr Opin Chem Eng. 2012;1:290-295.

[3] Fan L-S, Zeng L, Wang W, Luo S. Chemical looping processes for CO_2 capture and carbonaceous fuel conversion – prospect and opportunity. Energy Environ Sci. 2012;5:7254-7280.

[4] Adanez J, Abad A, Garcia-Labiano F, Gayan P, de Diego LF. Progress in chemical-looping combustion and reforming technologies. Prog Energy Combust Sci. 2012;38:215-282.

[5] Jin H, Hong H, Han T. Progress of energy system with chemical-looping combustion. Chin Sci Bull. 2009;54:906-919.

[6] Richter HJ, Knoche KF. Reversibility of combustion processes. Efficiency and Costing: American Chemical Society; 1983. p. 71-85.

[7] Ishida M, Zheng D, Akehata T. Evaluation of a chemical-looping-combustion power-generation system by graphic exergy analysis. Energy. 1987;12:147-154.

[8] Kim HR, Wang D, Zeng L, Bayham S, Tong A, Chung E, Kathe MV, Luo S, McGiveron O, Wang A, Sun Z, Chen D, Fan L-S. Coal direct chemical looping combustion process: Design and operation of a 25-kWth sub-pilot unit. Fuel. 2013;108:370-384.

[9] Sorgenfrei M, Tsatsaronis G. Design and evaluation of an IGCC power plant using iron-based syngas chemical-looping (SCL) combustion. Appl Energy. 2014;113:1958-1964.

[10] Jiménez Álvaro Á, Paniagua IL, Fernández CG, Carlier RN, Martín JR. Energetic analysis of a syngas-fueled chemical-looping combustion combined cycle with integration of carbon dioxide sequestration. Energy. 2014;76:694-703.

[11] Fan J, Hong H, Zhu L, Wang Z, Jin H. Thermodynamic evaluation of chemical looping combustion for combined cooling heating and power production driven by coal. Energy Convers Manage. 2017;135:200-211.

[12] Fan J, Lin Z, Hui H, Jiang Q, Jin H. A thermodynamic and environmental performance of in-situ gasification of chemical looping combustion for power generation using ilmenite with different coals and comparison with other coal-driven power technologies for CO_2 capture. Energy. 2017;119:1171-1180.

[13] Adánez J, Abad A, Mendiara T, Gayán P, de Diego LF, García-Labiano F. Chemical looping combustion of solid fuels. Prog Energy Combust Sci. 2018;65:6-66.

[14] Luo M, Yi Y, Wang C, Liu K, Pan J, Wang Q. Energy and exergy analysis of power generation systems with chemical‐looping combustion of coal. Chem Eng Technol. 2018;41:776-787.

[15] Mishra N, Bhui B, Vairakannu P. Comparative evaluation of performance of high and low ash coal fuelled chemical looping combustion integrated combined cycle power generating systems. Energy. 2019;169:305-318.

[16] Prabu V. Integration of in-situ CO_2-oxy coal gasification with advanced power generating systems performing in a chemical looping approach of clean combustion. Appl Energy. 2015;140:1-13.

[17] Ma J, Zhao H, Tian X, Wei Y, Rajendran S, Zhang Y, Bhattacharya S, Zheng C. Chemical looping combustion of coal in a 5kW_{th} interconnected fluidized bed reactor using hematite as oxygen carrier. Appl Energy.

2015;157:304-313.
[18] Adnan MA, Azis MM, Quddus MR, Hossain MM. Integrated liquid fuel based chemical looping combustion-parametric study for efficient power generation and CO_2 capture. Appl Energy. 2018;228:2398-2406.
[19] Chen L, Kong L, Bao J, Combs M, Nikolic HS, Fan Z, Liu K. Experimental evaluations of solid-fueled pressurized chemical looping combustion – The effects of pressure, solid fuel and iron-based oxygen carriers. Appl Energy. 2017;195:1012-1022.
[20] Zhang S, Xiao R, Zheng W. Comparative study between fluidized-bed and fixed-bed operation modes in pressurized chemical looping combustion of coal. Appl Energy. 2014;130:181-189.
[21] Fernández JR, Abanades JC. Conceptual design of a Ni-based chemical looping combustion process using fixed-beds. Appl Energy. 2014;135:309-319.
[22] Liu F, Ma J, Feng X, Wang Y. Simultaneous integrated design for heat exchanger network and cooling water system. Appl Therm Eng. 2018;128:1510-1519.
[23] Huang X, Lu P, Luo X, Chen J, Yang Z, Liang Y, Wang C, Chen Y. Synthesis and simultaneous MINLP optimization of heat exchanger network, steam Rankine cycle, and organic Rankine cycle. Energy. 2020;195.
[24] Fard MM, Pourfayaz F. Advanced exergy analysis of heat exchanger network in a complex natural gas refinery. J Cleaner Prod. 2019;206:670-687.
[25] Yong JY, Varbanov PS, Klemeš JJ. Heat exchanger network retrofit supported by extended Grid Diagram and heat path development. Appl Therm Eng. 2015;89:1033-1045.
[26] Konur O, Saatcioglu OY, Korkmaz SA, Erdogan A, Colpan CO. Heat exchanger network design of an organic Rankine cycle integrated waste heat recovery system of a marine vessel using pinch point analysis. Int J Energy Res. 2020;44:12312-12328.
[27] Zhang D, Lv D, Yin C, Liu G. Combined pinch and mathematical programming method for coupling integration of reactor and threshold heat exchanger network. Energy. 2020;205.
[28] Feng X, Zhu XX. Combining pinch and exergy analysis for process modifications. Appl Therm Eng. 1997;17:249-261.
[29] Mehdizadeh-Fard M, Pourfayaz F, Mehrpooya M, Kasaeian A. Improving energy efficiency in a complex natural gas refinery using combined pinch and advanced exergy analyses. Appl Therm Eng. 2018;137:341-355.
[30] Arriola-Medellín A, Manzanares-Papayanopoulos E, Romo-Millares C. Diagnosis and redesign of power plants using combined Pinch and Exergy Analysis. Energy. 2014;72:643-651.
[31] Shivaee-Gariz R, Tahouni N, Panjeshahi MH, Abbasi M. Development of a new graphical tool for calculation of exergy losses to design and optimisation of sub-ambient processes. J Cleaner Prod. 2020;275.
[32] Njoku HO, Egbuhuzor LC, Eke MN, Enibe SO, Akinlabi EA. Combined pinch and exergy evaluation for fault analysis in a steam power plant heat exchanger network. J Energy Resour Technol. 2019;141:122001.122001-122001.122010.
[33] Jie X, Zhao H, Meng C, Zheng C. Simulation study of an 800 MWe oxy-combustion pulverized-coal-fired power plant. Energy Fuels. 2011;25:2405-2415.
[34] Spinelli M, Peltola P, Bischi A, Ritvanen J, Hyppänen T, Romano MC. Process integration of chemical looping combustion with oxygen uncoupling in a coal-fired power plant. Energy. 2016;103:646-659.

[35] Zhu L, He Y, Li L, Wu P. Tech-economic assessment of second-generation CCS: Chemical looping combustion. Energy. 2018;144:915-927.

[36] Luo X, Wang M, Oko E, Okezue C. Simulation-based techno-economic evaluation for optimal design of CO_2 transport pipeline network. Appl Energy. 2014;132:610-620.

[37] Liu X, Yang S, Hu Z, Qian Y. Simulation and assessment of an integrated acid gas removal process with higher CO_2 capture rate. Comput Chem Eng. 2015;83:48-57.

[38] Romeo LM, Bolea I, Lara Y, Escosa JM. Optimization of intercooling compression in CO_2 capture systems. Appl Therm Eng. 2009;29:1744-1751.

[39] Olaleye AK, Wang M, Kelsall G. Steady state simulation and exergy analysis of supercritical coal-fired power plant with CO_2 capture. Fuel. 2015;151:57-72.

[40] Li F, Zeng L, Fan L-S. Biomass direct chemical looping process: Process simulation. Fuel. 2010;89:3773-3784.

[41] Bayham SC, Kim HR, Wang D, Tong A, Zeng L, McGiveron O, Kathe MV, Chung E, Wang W, Wang A. Iron-based coal direct chemical looping combustion process: 200-h continuous operation of a 25-kWth subpilot unit. Energy & fuels. 2013;27:1347-1356.

[42] Kim HR, Wang D, Zeng L, Bayham S, Tong A, Chung E, Kathe MV, Luo S, McGiveron O, Wang A. Coal direct chemical looping combustion process: Design and operation of a 25-kWth sub-pilot unit. Fuel. 2013;108:370-384.

[43] Jackson S, Brodal E. Optimization of the energy consumption of a carbon capture and sequestration related carbon dioxide compression processes. Energies. 2019;12:1603.

[44] DOE/NETL. Cost and performance baseline for fossil energy plants volume 1a: Bituminous coal (PC) and natural gas to electricity 2015. 2015; https://www.netl.doe.gov/. [accessed July, 30 2019].

[45] Xiong J, Zhao H, Zheng C. Exergy analysis of a 600 MWe oxy-combustion pulverized-coal-fired power plant. Energy Fuels. 2011;25:3854-3864.

[46] Do TX, Lim Y-i, Yeo H, Lee U-d, Choi Y-t, Song J-h. Techno-economic analysis of power plant via circulating fluidized-bed gasification from woodchips. Energy. 2014;70:547-560.

[47] Yi Q, Li W, Zhang X, Feng J, Zhang J, Wu J. Tech-economic evaluation of waste cooking oil to bio-flotation agent technology in the coal flotation industry. J Cleaner Prod. 2015;95:131-141.

[48] Huang Y, Zhao Y-J, Hao Y-H, Wei G-Q, Feng J, Li W-Y, Yi Q, Mohamed U, Pourkashanian M, Nimmo W. A feasibility analysis of distributed power plants from agricultural residues resources gasification in rural China. Biomass Bioenergy. 2019;121:1-12.

[49] Hsieh T-L, Xu D, Zhang Y, Nadgouda S, Wang D, Chung C, Pottimurphy Y, Guo M, Chen Y-Y, Xu M, He P, Fan L-S, Tong A. 250 kWth high pressure pilot demonstration of the syngas chemical looping system for high purity H2 production with CO2 capture. Applied Energy. 2018;230:1660-1672.

[50] Huang Y, Chu Q, Yi Q, Li W-Y, Xie K-C, Sun Q-W, Feng J. Feasibility analysis of high–low temperature Fischer–Tropsch synthesis integration in olefin production. Chem Eng Res Des. 2018;131:92-103.

[51] BP. Energy Outlook. 2019; https://www.bp.com/en/global/corporate/energy-economics/energy-outlook.html. [accessed July, 30 2019].

[52] China's electricity Price Supervision report 2018. 2019.

[53] Ye B, Jiang J, Zhou Y, Liu J, Wang K. Technical and economic analysis of amine-based carbon capture and sequestration at coal-fired power plants. J Cleaner Prod. 2019;222:476-487.

[54] Guo Z, Wang Q, Fang M, Luo Z, Cen K. Thermodynamic and economic analysis of polygeneration system integrating atmospheric pressure coal pyrolysis technology with circulating fluidized bed power plant. Appl Energy. 2014;113:1301-1314.

[55] Xiong J, Zhao H, Chen M, Zheng C. Simulation and exergy analysis of a 600 MWe oxy-combustion pulverized coal-fired power plant. In: Qi H, Zhao B, editors. Cleaner Combustion and Sustainable World. Berlin, Heidelberg: Springer Berlin Heidelberg; 2013. p. 1195-1199.

[56] Meerman JC, Ramírez A, Turkenburg WC, Faaij APC. Performance of simulated flexible integrated gasification polygeneration facilities. Part A: A technical-energetic assessment. Renewable and Sustainable Energy Reviews. 2011;15:2563-2587.

[57] Sun Y, Huang H, Vardhan H, Aguila B, Zhong C, Perman JA, Al-Enizi AM, Nafady A, Ma S. Facile approach to graft ionic liquid into MOF for improving the efficiency of CO_2 chemical fixation. ACS Appl Mater Interfaces. 2018;10:27124-27130.

[58] Cormos C-C. Oxy-combustion of coal, lignite and biomass: A techno-economic analysis for a large scale carbon capture and storage (CCS) project in Romania. Fuel. 2016;169:50-57.

[59] Porrazzo R, White G, Ocone R. Techno-economic investigation of a chemical looping combustion based power plant. Faraday Discuss. 2016;192:437-457.

[60] Lyngfelt A, Linderholm C. Chemical-looping combustion of solid fuels – technology overview and recent operational results in 100 kW unit. Energy Procedia. 2014;63:98-112.

[61] INC. AP. Greenhouse gas emissions control by oxygen firing in circulating fluidized bed boilers phase 1--A preliminary systems evaluation 2003. 2003. [accessed May, 15 2019].

[62] Tola V, Pettinau A. Power generation plants with carbon capture and storage: A techno-economic comparison between coal combustion and gasification technologies. Appl Energy. 2014;113:1461-1474.

[63] Xiao R, Song Q, Song M, Lu Z, Zhang S, Shen L. Pressurized chemical-looping combustion of coal with an iron ore-based oxygen carrier. Combust Flame. 2010;157:1140-1153.

[64] Osman M, Zaabout A, Cloete S, Amini S. Experimental demonstration of pressurized chemical looping combustion in an internally circulating reactor for power production with integrated CO_2 capture. Chem Eng J. 2020;401.

[65] Bhui B, Vairakannu P. Experimental and kinetic studies on in-situ CO_2 gasification based chemical looping combustion of low ash coal using Fe2O3 as the oxygen carrier. J CO_2 Util. 2019;29:103-116.

[66] Lyngfelt A, Leckner B, Mattisson T. A fluidized-bed combustion process with inherent CO_2 separation; application of chemical-looping combustion. Chem Eng Sci. 2001;56:3101-3113.

[67] Jerndal E, Leion H, Axelsson L, Ekvall T, Hedberg M, Johansson K, Källén M, Svensson R, Mattisson T, Lyngfelt A. Using low-cost iron-based materials as oxygen carriers for chemical looping combustion. Oil Gas Sci Technol. 2011;66:235-248.

[68] Moghtaderi B. Review of the recent chemical looping process developments for novel energy and fuel applications. Energy Fuels. 2012;26:15-40.

[69] Bhui B, Vairakannu P. Experimental and kinetic studies on in-situ CO_2 gasification based chemical looping combustion of low ash coal using Fe_2O_3 as the oxygen carrier. J CO_2 Util. 2019;29:103-116.

[70] Shen L, Wu J, Xiao J, Song Q, Xiao R. Chemical-looping combustion of biomass in a 10 kWth reactor with iron oxide as an oxygen carrier. Energy Fuels. 2009;23:2498-2505.

[71] Pettinau A, Ferrara F, Tola V, Cau G. Techno-economic comparison between different technologies for CO_2-free power generation from coal. Appl Energy. 2017;193:426-439.

[72] Atsonios K, Panopoulos K, Grammelis P, Kakaras E. Exergetic comparison of CO_2 capture techniques from solid fossil fuel power plants. Int J Greenhouse Gas Control. 2016;45:106-117.

[73] Jin H, Wang B. Principle of cascading utilization of chemical energy. J Eng Thermophys. 2004;25:181-184.

[74] Yan Q, Lu T, Luo J, Hou Y, Nan X. Exergy cascade release pathways and exergy efficiency analysis for typical indirect coal combustion processes. Combust Theory Modell. 2019;23:1134-1139.